Chemical Physics 72 (1982) 363–369
North-Holland Publishing Company

RANDOM COUPLING MODELS. IV. NUMERICAL INVESTIGATION OF THE DEPENDENCE ON THE RANDOM COUPLING DISTRIBUTION AND ON THE INITIAL PHASES

Benny CARMELI, Roberto TULMAN, Abraham NITZAN
Department of Chemistry, Tel-Aviv University, Tel Aviv 69978, Israel

and

M.H. KALOS
Courant Institute of Mathematical Sciences, New York University, 251 Mercer St., New York, NY 10012, USA

Received 12 April 1982

Results of numerical simulations of the time evolution associated with hamiltonians characterized by random coupling matrix elements between dense manifolds of states are presented. It is shown that in the statistical limit (averaged magnitude of the coupling larger than the inverse density of states) the time evolution is independent of the detailed nature of the coupling and depends only on the first and second moments of the random coupling distribution, provided that these moments are finite. If these moments do not exist the golden rule is not obeyed. In the symmetric random coupling model the time evolution is independent of the choice of the initial phases.

1. Introduction

In a recent series of papers [1–6] we have investigated the spectral and dynamical behavior of systems described by (a) a dense energy level structure and (b) random coupling elements between these levels. The random coupling models (RCMs) are characterized by the energy level densities $\rho(E)$ and by the distribution $\mathcal{P}(V)$ of coupling matrix elements. A typical model is displayed in fig. 1. The dense manifolds $0, 1, 2, \ldots I, \ldots$ consist of states ($\{|0\alpha\rangle\}$ say for the manifold 0) which are eigenstates of some zero-order hamiltonian H_0. Information on the residual coupling V is provided through the distribution $\mathcal{P}(V)$ of the coupling elements $V_{I\alpha,J\beta}$ (I, J are manifold indices while α, β denote individual levels within such manifold) which are assumed to be random functions of the indices α and β. The model of fig. 1 has been successfully used (with $V_{I\alpha,J\beta}$ zero unless $J = I \pm 1$) to describe the kinetic behavior associated with infrared multiphoton excitation of large molecules [2,4,7,8]. Similar random coupling models have been used for other problems involving intramolecular processes in large molecules [9–13]. Random hamiltonians are encountered in many branches of physics (e.g. in the theory of nuclear spectra [14] and in theories of random solids [15]). The typical feature in large molecule dynamics is that processes of interest involve transitions between manifolds of states as in fig. 1.

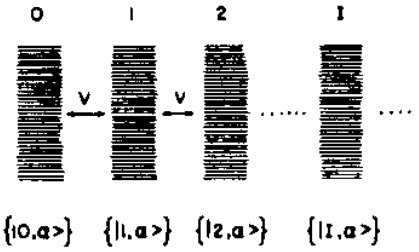

Fig. 1. A schematic model of coupled manifolds of levels.

The purpose of the present paper is to supplement our previous work on the time evolution associated with such RCMs by further computer simulation results aimed at strengthening some of our conclusions on the effect of the nature of the distribution $\mathcal{P}(V)$ on the resulting dynamical behavior. In addition, we present some computer simulations which examine

0301-0104/82/0000–0000/$ 02.75

the role played by the nature of the initial state (the combination of states from the manifold 0) on the subsequent time evolution.

2. A review of the model and its implications

Our model is described by fig. 1, where the coupling matrix elements $V_{I\alpha,J\beta}$ are assumed to be real random functions of the state indices α and β. In the present work we assume that no correlation exists between $V_{I\alpha,J\beta}$ elements with different α and/or β [‡], so that the distribution $\mathcal{P}(V)$ completely determines the statistical properties of the coupling elements. We note in passing that $\mathcal{P}(V)$ may, in principle, depend on the indices I and J. The average

$$\langle V\rangle_{I,J} = \frac{1}{NN'}\sum_{\alpha}\sum_{\alpha'} V_{I\alpha,J\alpha'} = \int \mathrm{d}V\, V\, \mathcal{P}_{IJ}(V) \qquad (1)$$

(N and N' being the number of levels contributing to the α and α' sums, respectively) is the first of the moments $\langle V^n\rangle_{I,J} = \int \mathrm{d}V\, V^n\, \mathcal{P}_{I,J}(V)$, which determine the distribution $\mathcal{P}_{I,J}(V)$. It is convenient to define

$$U_{I,J} = \langle V\rangle_{I,J} \qquad (2)$$

and

$$v_{I\alpha,J\beta} = V_{I\alpha,J\beta} - U_{I,J}\ . \qquad (3)$$

The assumption of no correlation stated above implies that

$$\langle v_{I\alpha,I'\alpha'} v_{J\beta,J'\beta'}\rangle = \langle v^2\rangle_{I,I'}(\delta_{I,J}\delta_{I',J'}\delta_{\alpha,\beta}\delta_{\alpha',\beta'} + \delta_{I,J'}\delta_{I',J}\delta_{\alpha,\beta'}\delta_{\alpha',\beta})\ . \qquad (4)$$

It should be pointed out that the averages defined in (4) or in the first equality of (1) are coarse grained averages which involve the levels within some energy interval ϵ. These averages may still depend on the energy E (which is equivalent to saying that $\mathcal{P}_{IJ}(V)$ may depend on E). If ΔE is the energy scale for this dependence (e.g. $\Delta E \approx (\mathrm{d}\ln\langle v^2\rangle/\mathrm{d}E)^{-1}$), τ is the timescale of the experiment, ϵ our energy resolution and ρ the density of states in a given manifold, the following inequalities are assumed to hold

$$\hbar\rho \gg \hbar/\epsilon \gg \tau \gg \hbar/\Delta E\ . \qquad (5)$$

A more detailed presentation of the model and the associated assumptions is given in paper I [3]. With models characterized by the inequalities (5) numerical simulations [5] have led to two important conclusions:

(a) The physical observables of the system depend only on the distributions $\mathcal{P}_{IJ}(V)$ and not on the detailed choice of coupling elements $V_{I\alpha,J\beta}$. In other words, two different sets of coupling elements which are characterized by the same average properties (moments) lead to the same observables of interest, e.g. the time evolution on the relevant timescale τ.

(b) Noting that the distribution $\mathcal{P}(V)$ is characterized in principle by an infinite number of moments $\langle V^n\rangle$, a remarkable property of systems characterized by the inequalities (5) is that the observables of interest depend only on the two lowest moments $\langle V\rangle = u$ and $\langle v^2\rangle = \langle V^2\rangle - u^2$ of the distribution.

Assuming the validity of conclusions (a) and (b) we were able to focus on the particular RCM with gaussian distribution (characterized by its two lowest moments), and within the gaussian RCM we have shown that the model of fig. 1 (with one initial state $|0\rangle$) leads to a time evolution of the manifold populations $P_I(t) = \Sigma_\alpha P_{I\alpha}(t)$, described by

$$\dot{P}_I(t) = \sum_J [k_{I,J}P_J(t) - k_{J,I}P_I(t)]\ , \qquad (6)$$

where the main contribution to the rates comes from the variance $\langle v^2\rangle$

$$k_{I,J} = 2\pi\langle v^2\rangle_{I,J}\rho_I\ , \qquad (7)$$

with other much smaller contributions [‡] which depend on u (see paper I for details). It should be noticed that eq. (7) differs from the usual golden rule result in that $\langle v^2\rangle = \langle V^2\rangle - \langle V\rangle^2$ appears instead of $\langle V^2\rangle$.

The numerical simulations reported below are designed to provide more information regarding the range of validity of conclusion (b) above. In addition, we generalise our earlier computations by using an initial state of the form $\Sigma_\alpha C_\alpha|0\alpha\rangle$ and study the effect of the nature of this initial superposition on the subsequent time evolution. Throughout this paper we employ dimensionless units with $\hbar = 1$.

[‡] See ref. [1] for a treatment of correlations.

[‡] The u-dependent contributions are much smaller than the v-dependent ones if u and $\langle v^2\rangle^{1/2}$ are of the same order.

3. Dependence on the distribution of matrix elements

In paper III we have carried out simulations on the time evolution associated with the model displayed in fig. 1 for the case where the manifold 0 contains a single level. This level $|0\rangle$ is the initial state of the system. We have followed the populations of the manifolds 0,1,2, ... and have shown that the time evolution agrees with the kinetic equations obtained for this model for the gaussian random coupling model. Having obtained identical (within small statistical differences) results using gaussian, rectangular and bimodal distributions for the coupling matrix elements (with parameters chosen so that all these distributions have the same first and second moments) we have concluded that under the model assumptions outlined in section 2, the time evolution is governed by only the first two moments of the distribution of coupling matrix elements.

In what follows we present the results of additional numerical simulations which support this conclusion. We employ random distributions given by ☆

$$\mathcal{P}_n(V) = 0\,, \qquad |V| < a_n\,;$$

$$= \tfrac{1}{2}(n-1)|V|^{-n}\,, \quad |V| \geqslant a_n\,, \tag{8}$$

where the parameter a is chosen to yield the prescribed second moment

$$a_n = \{[(n-3)/(n-1)]\langle V^2\rangle\}^{1/2}\,. \tag{9}$$

By using eq. (8) with different n to generate the matrix elements for the model of fig. 1, we can investigate the dependence of the time evolution on the nature of the distribution. To generate a sequence of coupling matrix elements which correspond to a given distribution $\mathcal{P}(V)$ we first form random numbers corresponding to a uniform distribution in the range $0 \leqslant x \leqslant 1$, then define $\mathcal{P}(V)$ by $\int_{-\infty}^{V} \mathrm{d}V\,\mathcal{P}(V) = x$. After generating the hamiltonian matrix in this way we solve numerically the Schrödinger equation to obtain the time evolution of the manifold populations. Each solution is referred to as a "trajectory".

Our results for all distributions for which the first and second moments are finite ($n > 3$) confirm our previously reached conclusions: (a) Under the conditions outlined in section 2 the time evolution is determined by the distribution and not by the particular choice of coupling matrix elements. This has been shown by running several trajectories for different choices of coupling elements (using the same distribution) and getting similar time evolution for all these trajectories. (b) The time evolution is determined only by the first and second moments $\langle V\rangle$ and $\langle V^2\rangle$ of the distribution and is not sensitive to the higher moments. Thus all distributions $\mathcal{P}_n(V)$ yield the same time evolution provided $\langle v^2\rangle$ and $u = \langle V\rangle$ are the same. We have verified this for $n = 4$–11. An example is shown in fig. 2. (c) The time evolution follows the kinetic equations derived in papers I and II. The equations are identical to the Pauli master equation for $u = 0$.

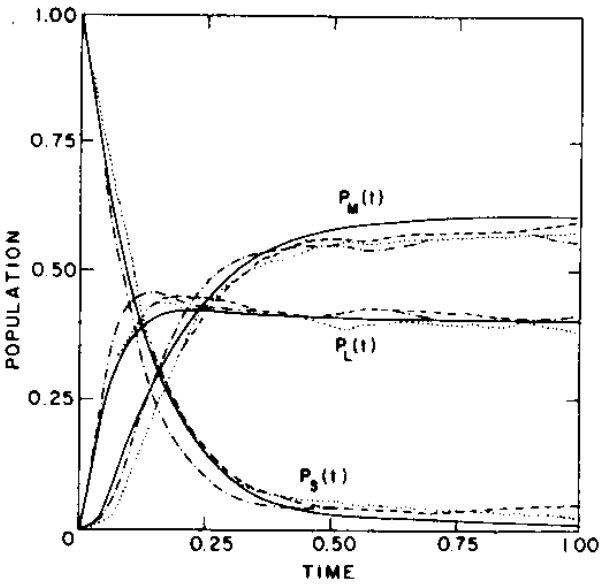

Fig. 2. Time evolution for the model in fig. 1 where the first manifold $\{|0,\alpha\rangle\}$ contains only one level and is coupled consecutively to two manifolds with state densities $\rho_1 = 1$, $\rho_2 = 1.5$. The total number of states taken in this simulation is 75 in each manifold. RCMs are characterized by $\langle V_{01}^2\rangle = 1.273$, $\langle V_{12}^2\rangle = 1.0$ and $\langle V\rangle = 0$. Solid line: analytical results [(eqs. (6) and (7)]; dashed line: gaussian distribution; dotted line: $\mathcal{P}_n(V)$ with $n = 7$ [cf. eq. (8)]; dotted–dashed line: $\mathcal{P}_n(V)$ with $n = 4$.

The situation is different when the distribution $\mathcal{P}(V)$ does not have finite first and/or second moment, e.g. $\mathcal{P}(V)$ of eq. (8) with $n = 2, 3$. Simulations based on these distributions show that:

(a) The time evolution is different for different sequences of coupling matrix elements, i.e. it is not determined by the distribution alone. This is seen in

☆ The distributions $\mathcal{P}_n(V)$ are characterized by zero first moments. To simulate a random coupling with a non-zero first moment it is sufficient to define $V = u + v$, where v is taken from eq. (8) and where $u = \langle V\rangle$.

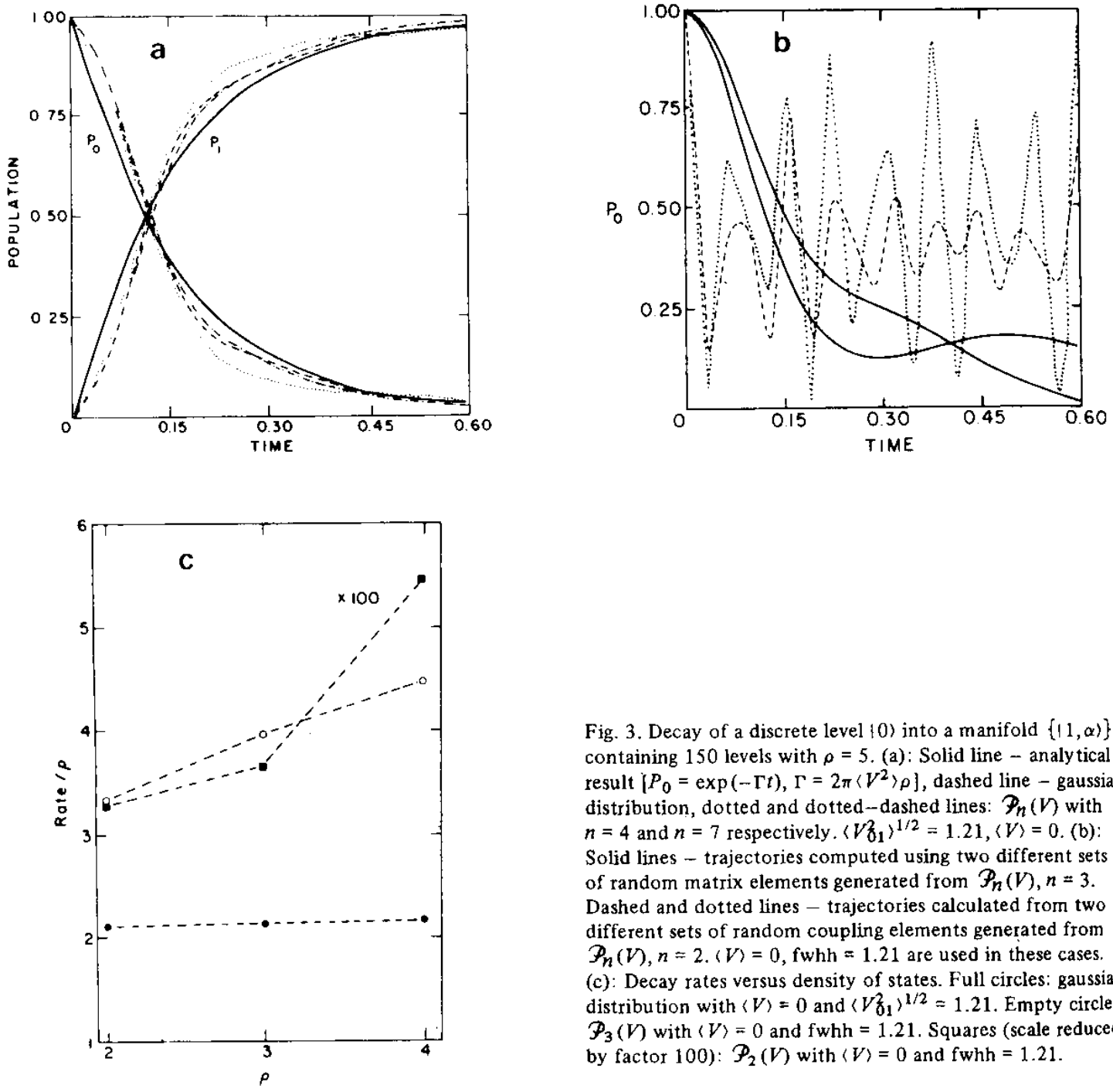

Fig. 3. Decay of a discrete level $|0\rangle$ into a manifold $\{|1,\alpha\rangle\}$ containing 150 levels with $\rho = 5$. (a): Solid line – analytical result [$P_0 = \exp(-\Gamma t)$, $\Gamma = 2\pi\langle V^2\rangle\rho$], dashed line – gaussian distribution, dotted and dotted–dashed lines: $\mathcal{P}_n(V)$ with $n = 4$ and $n = 7$ respectively. $\langle V_{01}^2\rangle^{1/2} = 1.21$, $\langle V\rangle = 0$. (b): Solid lines – trajectories computed using two different sets of random matrix elements generated from $\mathcal{P}_n(V)$, $n = 3$. Dashed and dotted lines – trajectories calculated from two different sets of random coupling elements generated from $\mathcal{P}_n(V)$, $n = 2$. $\langle V\rangle = 0$, fwhh = 1.21 are used in these cases. (c): Decay rates versus density of states. Full circles: gaussian distribution with $\langle V\rangle = 0$ and $\langle V_{01}^2\rangle^{1/2} = 1.21$. Empty circles: $\mathcal{P}_3(V)$ with $\langle V\rangle = 0$ and fwhh = 1.21. Squares (scale reduced by factor 100): $\mathcal{P}_2(V)$ with $\langle V\rangle = 0$ and fwhh = 1.21.

figs. 3a and 3b where the time evolution associated with the simplest model of a single initial level coupled to a dense manifold is displayed. We compare for this model the time evolution obtained for the gaussian random model and for $\mathcal{P}_n(V)$ $(n = 4, 7)$ with $u = 0$ and a given $\langle v^2\rangle$, to that associated with the $n = 2, 3$ models in which a_n was chosen to yield a full width at half height (fwhh) equal to the gaussian $\langle v^2\rangle^{1/2}$, i.e. $a_n = 2^{-(n+1)/n}\langle v^2\rangle^{1/2}$. In the first case (fig. 3a) the different distributions are seen to yield the same time evolution (within statistical differences that are expected to disappear when p becomes very large) *. This was also seen for different sets of cou-

* The different initial slopes observed in the analytical result as compared with the numerical simulations are "finite-size" effects caused by the finite energy extent (compared with the decay rate k) of the manifolds used in the simulations. This energy extent is given by N/ρ, where N and ρ are total number and density of levels in the manifold. The analytical result assumes $N/\rho \gg k$.

pling elements taken from the same distribution. In the second case (fig. 3b) the time evolution depends on the particular choice of coupling elements.

(b) As may be inferred from (a), the golden rule is not obeyed for the $n = 2, 3$ distributions. In fig. 3c we compare the decay rates calculated for a single level coupled to a dense manifold of levels for three cases which differ by the density of states ρ. According to the golden rule this rate should be proportional to ρ. This holds for the gaussian distribution while it is seen not to be the case for the $n = 2, 3$ distributions. The deviations become very large for the $n = 2$ distribution where most trajectories are obtained non-exponential.

We have also used a lorentzian distribution in several of the simulations and found its behavior to be qualitatively similar to that of the $n = 2$ distribution.

4. The effect of the nature of the initial state

The simulations described above, which are all based on a single initial level coupled to the $\{|1\alpha\rangle\}$ manifold are a special case of the situation where the initial state is an incoherent combination of states $\{|0\alpha\rangle\}$ given by the initial occupation probability for each such state. The results described above should then be averaged over this initial, diagonal density matrix.

Another situation which often arises in molecular physics problems is that where the initial state is a coherent superposition

$$\Psi(t = 0) = \sum_{\alpha} C_{0\alpha} \exp(i\phi_{\alpha})|0\alpha\rangle , \qquad (10)$$

where the $C_{0\alpha}$ are the magnitudes of the initial amplitudes and the ϕ_{α} are the corresponding phases. Quack [8] has suggested that the choice of initial phases should have a profound effect on the time evolution in models of the kind presented by fig. 1. While this is undoubtedly true in many physical situations, our results indicate that for random coupling models with properties summarized in section 2 and with $\langle V\rangle = 0$ the choice of initial phases is immaterial: The time evolution of the manifold populations given the initial state (10) is the same as that obtained from an initial diagonal density matrix given by $\rho_{0\alpha,0\beta} = C_{0\alpha}^2 \delta_{\alpha,\beta}$, as long as we use symmetric ($\langle V\rangle = 0$) and well-behaved ($n \geqslant 4$) coupling distributions functions.

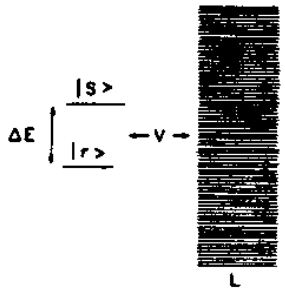

Fig. 4. A schematic model (two discrete levels $|r\rangle$ and $|s\rangle$ coupled to a manifold $\{|L,\alpha\rangle\}$) used to study the effect of initial phases.

As a simple example consider the model shown in fig. 4. We use the indices s and r to denote the two initial states and l to denote states of manifold L. The initial state is taken to be

$$\Psi(t = 0) = 2^{-1/2}\psi_s + 2^{-1/2}\, e^{i\phi}\psi_r . \qquad (11)$$

Fig. 5a shows the time evolution of the populations P_s, P_r and $P_L = \Sigma_l P_l$ for the constant coupling model $V_{sl} = V_{rl} = u$, for two different initial phases $\phi = 0$ and $\phi = \pi$. The evolution is seen to depend strongly on the initial phase. In contrast, in the corresponding RCM the time evolution does not depend on ϕ and is the same as that which is obtained from the initial diagonal density matrix, $\rho_{ss} = \rho_{rr} = 0.5$ (fig. 5b).

This behavior can easily be rationalized. Since $V_{sr} = 0$ the two states s and r "feel" each other only through their coupling to the manifold L. The quantity which determines their mutual interaction is the interference linewidth [16] which, for an infinite timescale experiment, is given by

$$\Gamma_{sr}(E) = 2\pi \sum_{l} V_{sl} V_{lr} \delta(E - E_l) . \qquad (12)$$

If the timescale of interest is τ, Γ_{sr} involves a sum over l states in an interval of order $\hbar/\tau$. When the conditions discussed in section 2 hold, this yields a finite result in the constant coupling case and practically zero in the RCM. Hence, in the RCM the r and s levels evolve as if they do not feel the presence of each other.

Similar results are obtained when the coupling between two dense manifolds is considered (fig. 6). Here we compare for the RCM (gaussian with $u = \langle V\rangle = 0$) the time evolution obtained for two cases:

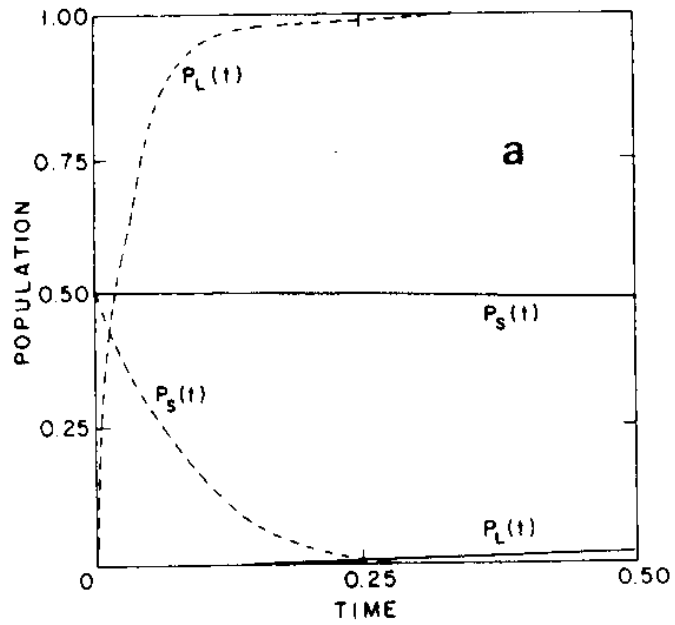

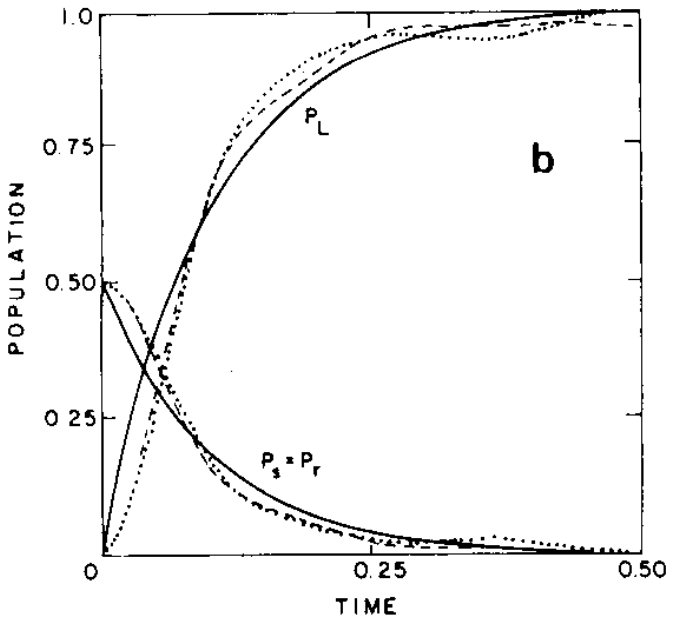

Fig. 5. Time evolution for the model described in fig. 4 with $\Delta E = 1, \rho_L = 2$. The total number of states in manifold L is 150 in this simulation. (a) Constant coupling elements $V_{SL} = V_{rL} = 1.262$. Solid line: $\phi = \pi$, dashed line: $\phi = 0$. (b) Same as (a) with random coupling elements chosen from a uniform distribution with $\langle V_{SL}^2 \rangle^{1/2} = \langle V_{rL}^2 \rangle^{1/2} = 1.262$ and $\langle V \rangle = 0$. Solid line: analytical result $[P_S(t) = P_S(0) \exp(-2\pi \langle V_{SL}^2 \rangle \rho_L t)$, $P_r(t) = P_r(0) \exp(-2\pi \langle V_{rL}^2 \rangle \rho_L t)]$; dashed line: uniformly distributed random initial phase within $(0, 2\pi)$; dotted line: constant initial phase $\phi = 0$.

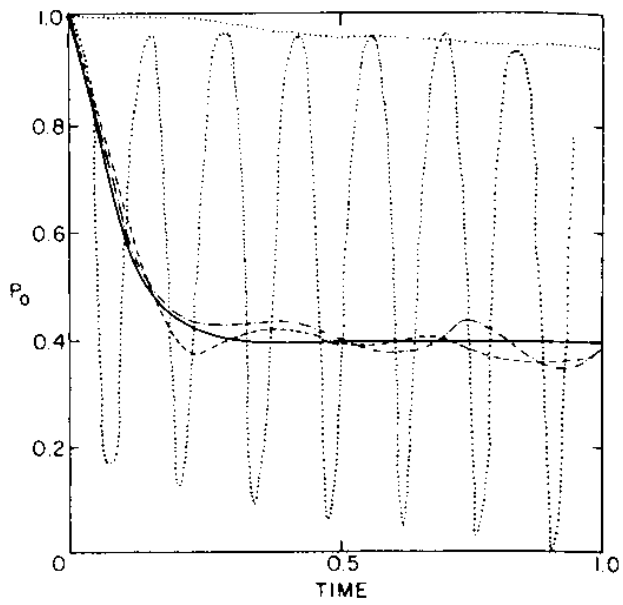

Fig. 6. Time evolution of the population in manifold $\{|0,\alpha\rangle\}$ which is coupled to a second manifold $\{|1,\alpha\rangle\}$. The density levels are $\rho_0 = 0.8333$ and $\rho_1 = 1.25$ and the total number of states is 75 in each manifold. Solid line: analytical result of the kinetic scheme (see text) with $k_{0\to1} = 2\pi \langle V_{01}^2 \rangle \rho_1 = 10$ and $k_{1\to0} = 2\pi \langle V_{01}^2 \rangle \rho_0 = 6.667$; dashed line: gaussian distribution with $\langle V_{01}^2 \rangle^{1/2} = 1.128$, $\langle V \rangle = 0$ and constant initial phases; dotted–dashed line: same with uniformly distributed initial phases within $(0, 2\pi)$; slowly decaying dotted line: constant coupling elements $V_{01} = 1.128$ with uniformly distributed intial phases; oscillating dotted line: constant coupling elements $V_{01} = 1.128$ and constant initial phases.

$$\Psi(t=0) = \sum_{\alpha} N^{-1/2} C_{0\alpha} \exp(i\phi_{0\alpha}) |0\alpha\rangle ,$$

one with all $\phi_{0\alpha}$ zero and the other where the $\phi_{0\alpha}$ are obtained from a uniform distribution in the range 0–2π. Within small statistical differences (which would disappear when the number of levels involved increases to infinity) the results are the same, and are identical to that which is obtained from the kinetic scheme

$$P_0 \underset{k_{01}}{\overset{k_{10}}{\rightleftharpoons}} P_1 ,$$

with $k_{10} = 2\pi \langle V^2 \rangle \rho_1$, and $k_{01} = 2\pi \langle V^2 \rangle \rho_0$. On the other hand, the constant coupling case is quite sensitive to the choice of initial phases. We note that the very slow time evolution observed in the constant coupling–random phase model is in agreement with a theoretical analysis given earlier #.

See appendix C in ref. [4].

5. Summary

By numerical simulations we have shown that the time evolution associated with inter-manifold random coupling models, in the statistical limit [characterized by the validity of the inequalities (5)] is governed by the nature of the distribution of coupling elements and in fact, only by the first two moments of this distribution. This holds, provided the distributions are well behaved in the sense that their first two moments $\langle V \rangle$ and $\langle V^2 \rangle$ are finite. When this is not so, the time evolution becomes sensitive to the particular realization of matrix elements, different sequences of such elements yield different temporal behavior. Oscillating, non-exponential and non-golden rule evolutions characterize these cases.

In the symmetric ($\langle V \rangle = 0$) RCM the time evolution is insensitive to the choice of initial phases: only the initial populations matter. In other cases, in particular in the CCM ($V = \langle V \rangle$) the time evolution is affected by interference between the initially populated levels and the choice of initial phases becomes important.

References

[1] B. Carmeli and A. Nitzan, Chem. Phys. Letters 58 (1978) 310.
[2] B. Carmeli and A. Nitzan, Chem. Phys. Letters 62 (1978) 457.
[3] B. Carmeli and A. Nitzan, J. Chem. Phys. 72 (1980) 2054 (referred to as paper I).
[4] B. Carmeli and A. Nitzan, J. Chem. Phys. 72 (1980) 2070 (referred to as paper II).
[5] B. Carmeli, I. Schek, A. Nitzan and J. Jortner, J. Chem. Phys. 72 (1980) 1928 (referred to as paper III).
[6] A. Nitzan and B. Carmeli, in: Lecture notes in physics, no. 132, Systems far from equilibrium, Proceedings, Sitges, Spain, 1980, ed. L. Garrido (Springer, Berlin, 1980).
[7] I. Schek and J. Jortner, J. Chem. Phys. 70 (1979) 3016.
[8] M. Quack, J. Chem. Phys. 69 (1978) 1282.
[9] W.M. Gelbart, S.A. Rice and K.F. Freed, J. Chem. Phys. 57 (1972) 4699;
K.G. Kay, J. Chem. Phys. 61 (1974) 5205.
[10] E.J. Heller and S.A. Rice, J. Chem. Phys. 61 (1978) 936.
[11] J.M. Delory and C. Tric, Chem. Phys. 3 (1974) 54.
[12] W.M. Gelbart, D.F. Heller and M.L. Elert, Chem. Phys. 7 (1975) 116.
[13] S.D. Druger, J. Chem. Phys. 67 (1977) 3238, 3249.
[14] E.P. Wigner, Ann. Math. Leipzig 62 (1955) 548; 67 (1958) 325;
T.A. Brody, J. Flores, J.B. French, P.A. Mello, A. Pandrey and S.S.M. Wong, Rev. Mod. Phys. 53 (1981) 385.
[15] R.T. Elliot, J.A. Krumhansl and P.L. Leath, Rev. Mod. Phys. 46 (1974) 465.
[16] A. Nitzan and J. Jortner, J. Chem. Phys. 57 (1972) 2870.